Ceramics International 51 (2025) 62836–62843

Contents lists available at ScienceDirect

Ceramics International

journal homepage: www.elsevier.com/locate/ceramint

Two-sample characterization of elastic and piezoelectric constants of piezoelectric materials via combination of ultrasonic pulse-echo, electric resonance, and hydrostatic piezoelectric constant measurements

Shanshan Sun [b], Youquan Chen [b], Shusheng Li [a,*], Ruoyu Jia [b], Ailing Xiao [b], Liguo Tang [b,c,d,**], Wenyu Luo [d,e]

[a] College of Aerospace and Civil Engineering, Harbin Engineering University, China
[b] Key Laboratory of Underwater Acoustic Communication and Marine Information Technology, Ministry of Education, College of Ocean and Earth Sciences, Xiamen University, Xiamen, 361010, China
[c] Shenzhen Research Institute of Xiamen University, Shenzhen, 518000, China
[d] State Key Laboratory of Acoustics and Marine Information, Institute of Acoustics, Chinese Academy of Sciences, Beijing, 100190, China
[e] University of Chinese Academy of Sciences, Beijing, 100049, China

ARTICLE INFO

Handling Editor: P. Vincenzini

Keywords:
Full matrix material constants
Piezoelectric materials
Ultrasonic pulse-echo method
Electric resonance method
Hydrostatic piezoelectric constant

ABSTRACT

The traditional electric resonance method typically requires at least five samples to characterize the elastic and piezoelectric constants (EPCs) of piezoelectric materials (PMs), which is likely to result in a self-consistency problem because sample-to-sample variation cannot be overcome. In general, a smaller number of samples produces better results. Resonant ultrasound spectroscopy can characterize the EPCs of PMs using only a single sample: however, this method requires PM samples with high mechanical quality factors. To reduce the number of samples required for characterization, this study combines the ultrasonic pulse-echo method, electric resonance method, and hydrostatic piezoelectric constant measurement to characterize the EPCs of PMs with ∞mm and 4mm point group symmetries. Only two samples—a rectangular block sample and thin-disk sample—are required to characterize the EPCs of the PMs with ∞mm point group symmetry, while that of the sample with 4mm point group symmetry requires only a rectangular block and long thin slice samples. The agreement between the measured electronic spectra of Fuji C64 lead zirconate titanate ceramics and $[001]_C$-poled $28Pb(In_{1/2}Nb_{1/2})O_3$–$43Pb(Mg_{1/3}Nb_{2/3})O_3$–$29PbTiO_3$ single crystals and those derived from the calculated PMs confirms the reliability of the method.

1. Introduction

Piezoelectric materials (PMs), such as piezoelectric lead zirconate titanate (PZT) ceramics, are commonly used in the fabrication of underwater sensors and actuators, nondestructive testing, and medical ultrasound applications. The full matrix material constants (FMMCs) of PMs, including their elastic, piezoelectric, and dielectric constants, must be characterized prior to their use in device fabrication. The elastic and piezoelectric constants (EPCs) of PMs are most commonly characterized using the electrical resonance (ER) method described in the IEEE piezoelectricity standard [1]. The EPCs of various piezoelectric ceramics and single crystals (SCs) have been characterized using the ER method [2–5]; however, this method typically requires at least five samples, which is likely to result in a self-consistency problem because the sample-to-sample variation cannot be overcome [6,7]. To ensure the self-consistency of the characterized results, the number of samples required for accurate characterization must be minimized; ideally using only one sample should be required. Sheritt et al. [8] introduced a procedure for characterizing the FMMCs of PMs with ∞mm symmetry from a single disk sample that was first used as the radial extensional (RE) and thickness extensional (TE) resonators. Subsequently, a length thickness extensional (LTE) resonator was cut from the disk. The electrodes were then removed and applied to another two surfaces to form a longitudinal shear resonator, which was then repolarized to form a

* Corresponding author.
** Corresponding author. Key Laboratory of Underwater Acoustic Communication and Marine Information Technology, Ministry of Education, College of Ocean and Earth Sciences, Xiamen University, Xiamen, 361010, China.
E-mail addresses: lissheu@126.com (S. Li), liguotang@xmu.edu.cn (L. Tang).

https://doi.org/10.1016/j.ceramint.2025.10.404
Received 21 August 2025; Received in revised form 5 October 2025; Accepted 28 October 2025
Available online 29 October 2025

length-extensional (LE) resonator. Five resonators were used for characterization. Because the samples were cut and repolarized, the results cannot be considered to originate from a single sample. Variations in the sample thickness may lead to inconsistent polarization levels.

In general, measuring all dielectric constants of PMs from one sample is straightforward; however, characterizing the EPCs of PMs using a single sample presents a considerable challenge. Although this can be accomplished using resonant ultrasound spectroscopy, this technique requires PMs with a high mechanical quality factor (Q_M) [9–12]. Combining the ER method with the ultrasonic pulse-echo (UPE) method, which characterizes some elastic constants of solid samples [1,13], enables the EPCs of PMs to be characterized. Zhang et al. [14] characterized the EPCs of $[001]_C$-poled $0.67Pb(Mg_{1/3}Nb_{2/3})O_3$–$0.33PbTiO_3$ (67PMN-33PT) SCs using a combination of the ER and UPE methods. Four samples were employed, including a rectangular block sample with the UPE method, and three other samples with the ER method. Liu et al. [15] characterized the EPCs of $[011]_C$-poled 72PMN-28PT SCs using the combination of the ER and UPE methods. During characterization, the characterization of $[011]_C$-poled relaxor-based SCs required more ER samples than that of $[001]_C$-poled relaxor-based SCs. The excellent piezoelectric properties of relaxor–based SCs are suitable for fabricating high-performance piezoelectric devices; however, piezoelectric ceramics, such as PZT ceramics, remain among the most common PMs used in practical applications. The precise characterization of FMMCs of various piezoelectric ceramics and relaxor-based SCs with high efficiency is therefore of considerable significance.

In this study, a two-sample method was developed to characterize the FMMCs of PMs with ∞mm and 4mm point symmetries. Low-Q_M Fuji C64 PZT and $[001]_C$-poled $28Pb(In_{1/2}Nb_{1/2})O_3$–$43\ Pb(Mg_{1/3}Nb_{2/3})O_3$–$29PbTiO_3$ (28PIN-43PMN-29PT) SCs were used as the characterization examples. The characterization of Fuji C64 PZT with ∞mm point symmetry required only a rectangular block sample (#1) and disk sample (#2). Numerous piezoelectric ceramics have the ∞mm point symmetry, including PZT, $BaTiO_3$, $Bi_4Ti_3O_{12}$, and $PbNb_2O_6$ ceramics. Moreover, only a rectangular block sample (#3) and a long thin slice sample (#4) were used for characterizing $[001]_C$-poled 28PIN-43PMN-29PT single crystals with 4mm point symmetry. The method described herein is also suitable for the characterization of high-Q_M PMs with ∞mm and 4mm symmetries.

2. Experimental procedures

2.1. Sample preparation

Cylindrical Fuji C64 PZT samples were provided by Fuji Ceramics Corporation. A rectangular block sample (#1) and a disk sample (#2) were cut from the same cylindrical sample using a Kejing STX-202A diamond wire cutting saw (Fig. 1). The $[001]_C$-poled 28PIN-43PMN-29PT samples were provided by the Shanghai Institute of Ceramics, China. A rectangular block sample (#3) and a long thin slice sample (#4) were used for characterization. All samples were ground using a Kejing UNIPOL-802 automatic grinding and polishing machine. The sample dimensions were measured using a Mikrometry DHG-050 digital micrometer (Table 1). The densities of the block samples were measured using an Xiongfa XF-120MD electronic densitometer (Table 2). The length, width, and height of the rectangular sample are denoted l_x, l_y, and l_z, respectively. The z-axis represents the polarization direction. The diameter and thickness of the disk sample are denoted Φ and h, respectively.

PZT ceramics have a ∞mm point symmetry. The elastic, piezoelectric, and dielectric matrices are formulated as in Equations (1)–(3):

$$[c] = \begin{bmatrix} c_{11}^E & c_{12}^E & c_{13}^E & 0 & 0 & 0 \\ c_{12}^E & c_{11}^E & c_{23}^E & 0 & 0 & 0 \\ c_{13}^E & c_{23}^E & c_{33}^E & 0 & 0 & 0 \\ 0 & 0 & 0 & c_{44}^E & 0 & 0 \\ 0 & 0 & 0 & 0 & c_{44}^E & 0 \\ 0 & 0 & 0 & 0 & 0 & \frac{c_{11}^E - c_{12}^E}{2} \end{bmatrix}, \tag{1}$$

$$[e] = \begin{bmatrix} 0 & 0 & 0 & 0 & e_{15} & 0 \\ 0 & 0 & 0 & e_{15} & 0 & 0 \\ e_{31} & e_{31} & e_{33} & 0 & 0 & 0 \end{bmatrix}, \tag{2}$$

$$[\varepsilon] = \begin{bmatrix} \varepsilon_{11}^S & 0 & 0 \\ 0 & \varepsilon_{11}^S & 0 \\ 0 & 0 & \varepsilon_{33}^S \end{bmatrix}. \tag{3}$$

The $[001]_C$-poled 28PIN-43PMN-29PT single crystals have a 4mm point symmetry. Their piezoelectric and dielectric matrices are described by Equations (2) and (3), respectively. The elastic matrix is

Table 1
Dimensions and density of the Fuji C64 PZT samples.

Rectangular block sample (#1)			Disk sample (#2)		ρ (kg/m^3)
l_x (mm)	l_y (mm)	l_z (mm)	Φ (mm)	h (mm)	
4.060	5.476	4.311	10.001	0.490	7790

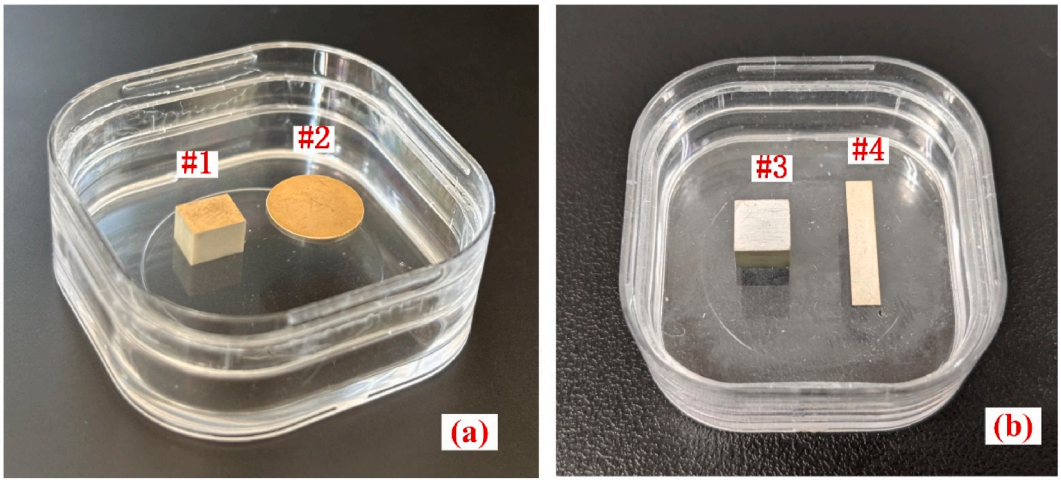

Fig. 1. Photographs of the samples. (a) Fuji C64 PZT; (b) $[001]_C$-poled 28PIN-43PMN-29PT single crystal.

Table 2
Dimensions and density of the $[001]_C$-poled 28PIN-43PMN-29PT samples.

Rectangular block sample (#3)			Long thin slice sample (#4)			ρ (kg/m^3)
l_x (mm)	l_y (mm)	l_z (mm)	l_x (mm)	l_y (mm)	l_z (mm)	
6.028	6.031	4.184	14.992	3.012	0.318	8158

given by Equation (4):

$$[c]=\begin{bmatrix} c_{11}^E & c_{12}^E & c_{13}^E & 0 & 0 & 0 \\ c_{12}^E & c_{11}^E & c_{23}^E & 0 & 0 & 0 \\ c_{13}^E & c_{23}^E & c_{33}^E & 0 & 0 & 0 \\ 0 & 0 & 0 & c_{44}^E & 0 & 0 \\ 0 & 0 & 0 & 0 & c_{44}^E & 0 \\ 0 & 0 & 0 & 0 & 0 & c_{66}^E \end{bmatrix}. \tag{4}$$

2.2. Measurement of dielectric constants

The capacitances of the rectangular block sample were measured using an HP4194 impedance analyzer and the free and clamped dielectric constants $\varepsilon_{11}^{\mathrm{T}}$, $\varepsilon_{11}^{\mathrm{S}}$, $\varepsilon_{33}^{\mathrm{T}}$, and $\varepsilon_{33}^{\mathrm{S}}$ were calculated using Equations (5)–(8), respectively:

$$\varepsilon_{11}^{\mathrm{T}}=\frac{C_{11}^{\mathrm{L}} l_x}{l_y l_z}, \tag{5}$$

$$\varepsilon_{11}^{\mathrm{S}}=\frac{C_{11}^{\mathrm{H}} l_x}{l_y l_z}, \tag{6}$$

$$\varepsilon_{33}^{\mathrm{T}}=\frac{C_{33}^{\mathrm{L}} l_z}{l_x l_y}, \tag{7}$$

$$\varepsilon_{33}^{\mathrm{S}}=\frac{C_{33}^{\mathrm{H}} l_z}{l_x l_y}, \tag{8}$$

where C_{11}^{L} and C_{11}^{H} are the low- and high-frequency capacitances along the x-axis, respectively, and C_{33}^{L} and C_{33}^{H} are the low- and high-frequency capacitances along the z-axis, respectively. The low- and high-frequency capacitances were measured at 1 kHz and 30 MHz, respectively.

2.3. UPE measurement

The UPE method was used to determine the elastic constants $\{c_{11}^{\mathrm{E}}, c_{33}^{\mathrm{D}}, c_{44}^{\mathrm{E}}, c_{44}^{\mathrm{D}}, c_{66}^{\mathrm{E}}\}$ of the rectangular sample, where c_{11}^{E} and c_{33}^{D} were obtained by measuring the velocities of longitudinal waves propagating along the x- and z-axes (L_x and L_z waves), respectively, c_{44}^{E}, c_{44}^{D}, and c_{66}^{E} were obtained by measuring the velocities of shear waves propagating along the z-axis (T_z wave), those propagating along the x-axis (or y-axis) and vibrating parallel to the z-axis ($T_x^{\parallel}$ wave), and those propagating along the x-axis (or y-axis) and vibrating perpendicular to the z-axis ($T_x^{\perp}$ wave), respectively. The c_{12}^{E} value of the Fuji C64 PZT sample was $c_{12}^{\mathrm{E}} = c_{11}^{\mathrm{E}} - 2c_{66}^{\mathrm{E}}$. The UPE measurement was performed using a CTS-8077PR pulse echoer connected to a Tektronix MDO3024 digital oscilloscope. UPE calculates a specific elastic constant c using the equation $c = \rho v^2$, where ρ and v are the density of the sample and velocity corresponding to each wave, respectively.

Based on the obtained ε_{11}^T, c_{44}^E, and c_{44}^D values, piezoelectric constants d_{15} and e_{15} were calculated using Equations (9) and (10), respectively:

$$d_{15}=\sqrt{\varepsilon_{11}^T\left(\frac{1}{c_{44}^E}-\frac{1}{c_{44}^D}\right)}, \tag{9}$$

$$e_{15}=d_{15}c_{44}^E. \tag{10}$$

2.4. Electric resonance measurement

The thin-disk sample of Fuji C64 PZT can be used as both a TE resonator and RE resonator. The electromechanical coupling coefficient k_{t}, elastic constants c_{33}^{D} and c_{33}^{E}, and piezoelectric constant e_{33} of the TE resonator can be calculated using Equations (11)–(14), respectively:

$$k_{\mathrm{t}}^2=\frac{\pi f_{\mathrm{r}}}{2f_{\mathrm{a}}}\tan\left(\frac{\pi(f_a-f_r)}{2f_a}\right), \tag{11}$$

$$c_{33}^{\mathrm{D}}=4\rho {l_{\mathrm{z}}}^2 f_{\mathrm{a}}^2, \tag{12}$$

$$c_{33}^{\mathrm{E}}=c_{33}^{\mathrm{D}}\left(1-k_{\mathrm{t}}^2\right), \tag{13}$$

$$e_{33}=k_t\sqrt{\varepsilon_{33}^S c_{33}^D}, \tag{14}$$

where f_r and f_a are the resonance and antiresonance frequencies of the TE resonator, respectively.

The properties of the thin-disk RE resonator, including the Poisson's ratio σ^{E}, elastic compliance constants s_{11}^E and s_{12}^E, planar electromechanical coupling factor k_p, transverse electromechanical coupling factor k_{31}, and piezoelectric strain constant d_{31}, were determined in accordance with an established procedure [16], which is summarized below.

The fundamental ($f_r^{(0)}$) and first overtone ($f_r^{(1)}$) resonance frequencies were measured using an HP4194 impedance analyzer, and σ^{E} was determined using Equation (15):

$$\frac{f_r^{(1)}}{f_r^{(0)}}=\frac{\xi_1}{\xi_0}\left[\frac{1+\frac{1}{3}(\sigma^E)^2h^2A_0(r,\xi_0)}{1+\frac{1}{3}(\sigma^E)^2h^2A_1(r,\xi_1)}\right]^{\frac{1}{2}}, \tag{15}$$

where r and h are the radius and thickness of the disk sample, respectively. ξ_0 and ξ_1 are the two minimum positive roots of

$$\xi J_0(\xi)=\left(1-\sigma^E\right)J_1(\xi), \tag{16}$$

where J_0 and J_1 are the zero- and first-order Bessel functions of the first kind, respectively. A_0 and A_1 are described by Equations (17) and (18), respectively:

$$A_0(r,\xi_0)=\frac{\left[\left({\xi_0}^2+1\right)J_0^2(\xi_0)+\left({\xi_0}^2-1\right)J_1^2(\xi_0)-1\right]}{{\xi_0}^2\left[J_0^2(\xi_0)+J_1^2(\xi_0)\right]-2\xi_0J_0(\xi_0)J_1(\xi_0)}\times\frac{{\xi_0}^2}{r^2}, \tag{17}$$

$$A_1(r,\xi_0)=\frac{\left[\left({\xi_1}^2+1\right)J_0^2(\xi_1)+\left({\xi_1}^2-1\right)J_1^2(\xi_1)-1\right]}{{\xi_1}^2\left[J_0^2(\xi_1)+J_1^2(\xi_1)\right]-2\xi_1J_0(\xi_1)J_1(\xi_1)}\times\frac{{\xi_1}^2}{r^2}. \tag{18}$$

The elastic compliance constants s_{11}^E and s_{12}^E were determined using Equations (19) and (20), respectively:

$$s_{11}^E=\frac{{\xi_1}^2}{\rho\pi^2(2r)^2(f_r)^2\left[1-(\sigma^E)^2\right]}, \tag{19}$$

$$s_{12}^E=-\sigma^E s_{11}^E. \tag{20}$$

Similarly, the electromechanical coupling factors k_p and k_{31} were determined using Equations (21) and (22), respectively:

$$\frac{k_p^2}{1-k_p^2}=\frac{(1-\sigma^E)J_1[\xi_1(1+\Delta f/f_r)]-\xi_1(1+\Delta f/f_r)J_0[\xi_1(1+\Delta f/f_r)]}{(1+\sigma^E)J_1[\xi_1(1+\Delta f/f_r)]}, \tag{21}$$

$$k_{31}^2 = \left(\frac{1-\sigma^E}{2}\right)k_p^2, \tag{22}$$

In addition, d_{31} was determined using Equation (23):

$$d_{31} = -k_p\sqrt{\varepsilon_{33}^T s_{11}^E (1-\sigma^E)/2}. \tag{23}$$

The long thin slice sample of $[001]_C$-poled 28PIN-43PMN-29PT can be used as a LTE resonator and as a TE resonator. The electromechanical coupling coefficient k_t, elastic constants c_{33}^D and c_{33}^E, and piezoelectric constant e_{33} of the TE resonator can be calculated using Equations (11)–(14), respectively. When used as the LTE resonator, s_{11}^E, k_{31}, and d_{31} can be calculated using Equations (24)–(26), respectively:

$$s_{11}^E = \frac{1}{4\rho l_x^2 f_r^2}, \tag{24}$$

$$-\frac{k_{31}^2}{1-k_{31}^2} = \frac{\pi f_a}{2f_r}\cot\left(\frac{\pi f_a}{2f_r}\right), \tag{25}$$

$$d_{31} = -\sqrt{k_{31}^2 \varepsilon_{33}^T s_{11}^E}. \tag{26}$$

2.5. Measurement of isostatic pressure piezoelectric constant d_h

Although d_{33} can be measured using a commercial d_{33} tester using the quasi-static method, this method exhibits low accuracy. In this study, the isostatic pressure piezoelectric constant d_h was measured using the system shown in Fig. 2. The samples were clamped using a fixer inside a sealed tank filled with silicone oil, which was pressurized using a high-pressure control system (Simingte SUPC-HD-1000) connected to an air compressor (Outstanding S1600 × 3). A quasi-static electric charge amplifier (Kistler 5015) was used to measure the variation in the electric charge. The static electric charge may shift over time and is therefore difficult to measure accurately. Increasing the time taken for the sealed tank to reach a specific pressure induces a larger error in the measurement of the electric charge: however, the sealed tank can depressurize rapidly. Therefore, to accurately measure the electric charge variation ΔQ, the sealed tank was pressurized to a given pressure, P_0, and then depressurized quickly. d_h was then calculated using Equation (27):

$$d_h = \frac{\Delta Q}{SP_0}, \tag{27}$$

where S is the area of the sample surface perpendicular to the polarization direction. Furthermore, d_{33} was calculated using $d_{33} = d_h - 2d_{31}$.

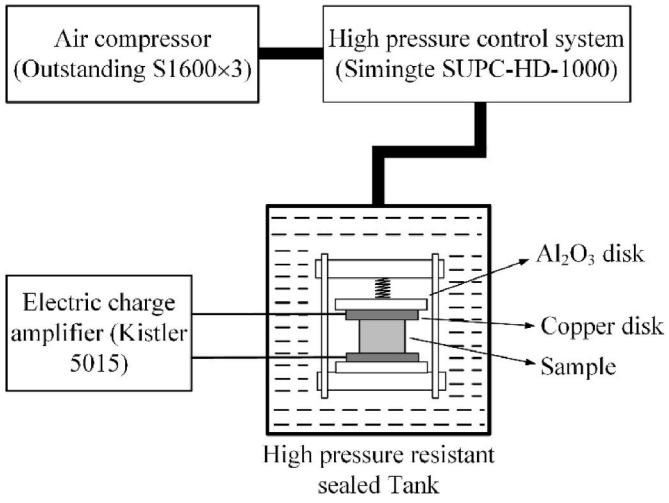

Fig. 2. d_h measurement apparatus.

2.6. Determination of c_{13}^E and e_{31} of ∞mm sample

The elastic constant c_{13}^E and piezoelectric constant e_{31} of the Fuji C64 PZT sample (with ∞mm point group symmetry) cannot be measured directly. Accordingly, the following procedure was used in this study to determine c_{13}^E and e_{31}. A reasonable range (a, b) of the value of c_{13}^E was initially selected. The elastic compliance matrix was then calculated using $s^E = [c^E]^{-1}$ by changing the value of c_{13}^E in intervals of 10 MPa. The calculated s_{11}^E and s_{12}^E values were compared with those of the RE resonator determined using the ER method. If they were consistent, the corresponding c_{13}^E value was taken as the determined value. Furthermore, e_{31} was calculated using Equation (28):

$$e_{31} = d_{31}\left(c_{11}^E + c_{12}^E\right) + d_{33}c_{13}^E. \tag{28}$$

2.7. Determination of c_{12}^E, c_{13}^E and e_{31} of 4mm sample

The elastic constants c_{12}^E, c_{13}^E and piezoelectric constant e_{31} of the $[001]_C$-poled 28PIN-43PMN-29PT sample (with 4mm point group symmetry) cannot be measured directly. The values of e_{31} and c_{13}^E were therefore calculated using Equations (29) and (30), respectively:

$$e_{31} = \frac{\varepsilon_{33}^T - \varepsilon_{33}^S - d_{33}e_{33}}{2d_{31}}, \tag{29}$$

$$c_{13}^E = \frac{e_{33} - d_{33}c_{33}^E}{2d_{31}}. \tag{30}$$

c_{12}^E was then calculated using Equation (31):

$$c_{12}^E = \frac{e_{31} - d_{31}c_{11}^E - d_{33}c_{13}^E}{d_{31}}. \tag{31}$$

3. Results and discussion

Figs. 3 and 4 show the ultrasonic pulse-echo waves propagating in the Fuji C64 PZT and $[001]_C$-poled 28PIN-43PMN-29PT single crystal block samples (#1 and #3), respectively. In contrast to electrical measurement methods, the UPE method is less sensitive to external factors and therefore provides more accurate measurements. The first two echoes corresponding to all waves can be clearly identified (Figs. 3 and 4), enabling the accurate measurement of the propagation times of different ultrasonic waves in the sample. Furthermore, the elastic constants $\{c_{11}^E, c_{33}^D, c_{44}^E, c_{44}^D, c_{66}^E\}$ can be accurately determined using UPE.

Fig. 5 shows the electric impedance spectra of the Fuji C64 PZT disk (#2) and the $[001]_C$-poled 28PIN-43PMN-29PT single crystal long thin slice (#4) samples. The electric resonance frequency (f_r) and anti-resonance frequency (f_a) were extracted from Fig. 5 and used to calculated various material constants (Eqs. (11)–(26)).

For the Fuji C64 PZT, the free and clamped dielectric constants of the Fuji C64 PZT were characterized using the method described in Section 2.2, while $\{c_{11}^E, c_{12}^E, c_{33}^D, c_{44}^E, c_{44}^D\}$ were characterized using the UPE method described in Section 2.3, d_{15} and e_{15} were obtained using Eqs. (9) and (10), $\{k_t, c_{33}^E, e_{33}\}$ and $\{\sigma^E, s_{11}^E, s_{12}^E, k_p, k_{31}, d_{31}\}$ were characterized via analysis of sample #2 as TE and RE resonators using the ER method, respectively, d_h was characterized using the method described in Section 2.5, and c_{13}^E and e_{31} were characterized using the procedure described in Section 2.6. Fuji Ceramics Corporation has provided the material constants of Fuji C64 PZT [17]. The piezoelectric strain constants d_{15}, d_{31}, and d_{33} are 670, –185, and 435 pC/N, respectively. The relative deviations between the values of d_{15}, d_{31}, and d_{33} provided by Fuji Ceramics Corporation and those obtained in this study are 5.4 %, 6.3 %, and 0.9 %, respectively. The electromechanical coupling coefficients k_{15}, k_{31}, k_{33}, k_t, and k_p provided by Fuji Ceramics Corporation are 0.71, 0.35, 0.73, 0.50, and 0.63, respectively; these values agree well with those in Table 3.

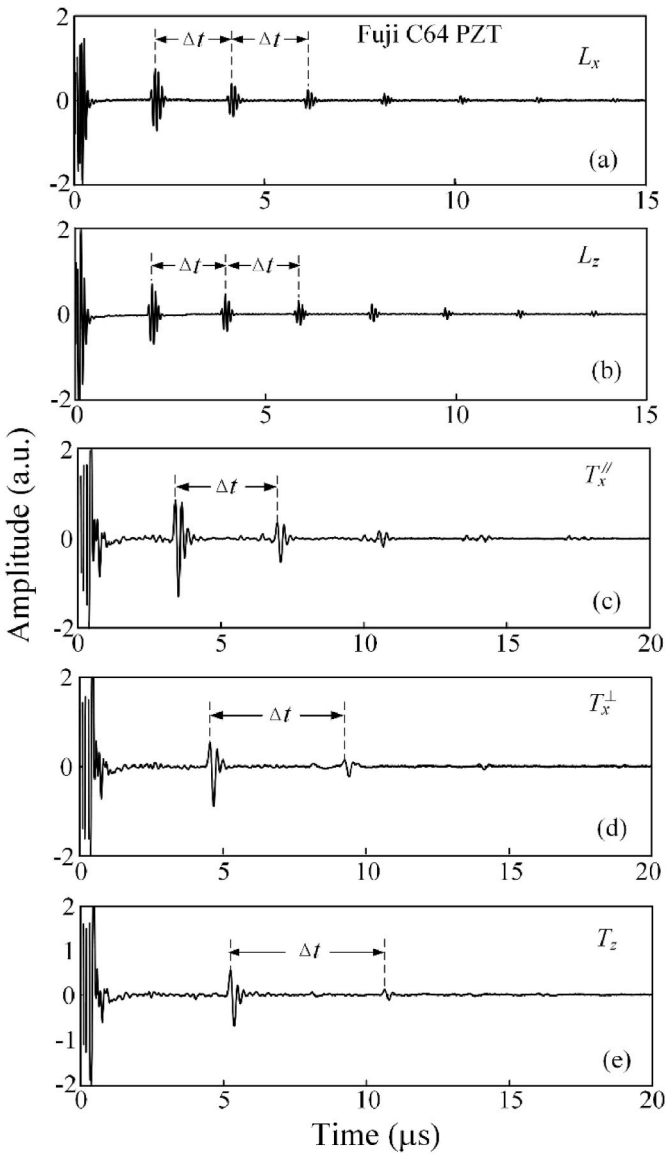

Fig. 3. Propagation of ultrasonic pulse-echo waves in the Fuji C64 PZT block sample (#1). (a) L_x; (b) L_z; (c) $T_x^{\parallel}$; (d) $T_x^{\perp}$; and (e) T_z waves.

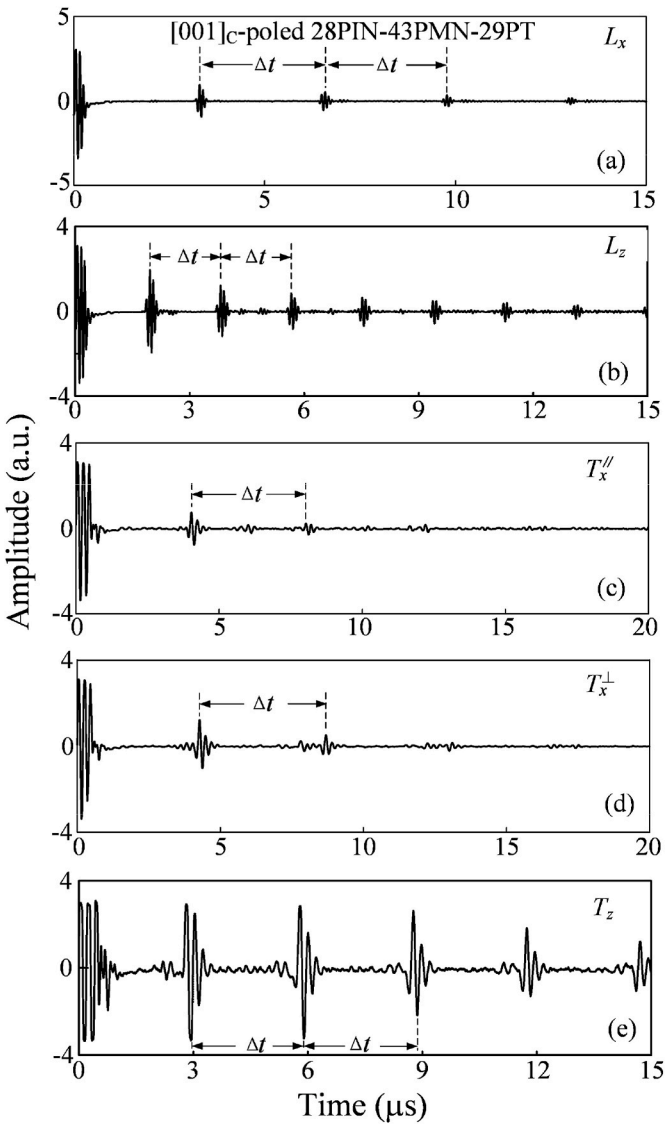

Fig. 4. Propagation of ultrasonic pulse-echo waves in the $[001]_C$-poled 28PIN-43PMN-29PT single crystal block sample (#3). (a) L_x; (b) L_z; (c) $T_x^{\parallel}$; (d) $T_x^{\perp}$; and (e) T_z waves.

Table 4 shows the characterized full matrix constants of the $[001]_C$-poled 28PIN-43PMN-29PT single crystals. The free and clamped dielectric constants were characterized using the method described in Section 2.2. Using the UPE method, $\{c_{11}^E, c_{33}^D, c_{44}^E, c_{44}^D, c_{66}^E\}$ were characterized, while d_{15} and e_{15} were characterized using Eqs. (9) and (10). Sample #4 was used as TE and LTE resonators: thus, $\{k_t, c_{33}^E, e_{33}\}$ and $\{s_{11}^E, k_{31}, d_{31}\}$ were characterized using the ER method. d_h was characterized using the method described in Section 2.5, while c_{12}^E, c_{13}^E and e_{31} were characterized using the procedure described in Section 2.7. Comparison of the characterization results of $[001]_C$-poled 28PIN-43PMN-29 PT SCs (Table 4) with those of $[001]_C$-poled 33PIN-38PMN-29 PT SCs [18] revealed that their elastic constants $\{c_{11}^E, c_{12}^E, c_{13}^E, c_{33}^E\}$ were remarkably close, with a maximum relative deviation of approximately 3.8 %. Moreover, their piezoelectric constants $\{e_{15}, e_{31}, e_{33}\}$ were also close. However, their dielectric constants $\{\varepsilon_{11}^T, \varepsilon_{33}^T, \varepsilon_{11}^S, \varepsilon_{33}^S\}$ exhibited significant differences. For example, the relative deviation between their ε_{11}^S values reached 45 %.

Thus, all elastic constants (c_{ij}^E) under a constant electric field, piezoelectric strain and stress constants (d_{ij} and e_{ij}), and free and clamped dielectric constants (ε_{ii}^T and ε_{ii}^S) of the Fuji C64 PZT and $[001]_C$-poled 28PIN-43PMN-29PT single crystals were successfully characterized. Other material constants, such as elastic constants c_{ij}^D and s_{ij}^D, can be readily obtained from equations expressing the relationship between different material constants, as shown in Tables 3 and 4

The relative errors were calculated to evaluate the accuracy of the results. The elastic constants c_{33}^D and c_{44}^D were calculated using Equations (25) and (26), respectively:

$$c_{33}^D = \frac{e_{33}^2}{\varepsilon_{33}^S} + c_{33}^E, \tag{25}$$

$$c_{44}^D = \frac{e_{15}^2}{\varepsilon_{11}^S} + c_{44}^E. \tag{26}$$

The calculated c_{33}^D and c_{44}^D values of the Fuji C64 PZT were 16.23×10^{10} and 3.846×10^{10} N/m^2, respectively. The relative errors between the calculated c_{33}^D values and those obtained using the UPE method (Table 3) and the ER method (16.19×10^{10} N/m^2) were approximately 4.4 % and 0.2 %, respectively. Moreover, the relative error between the calculated c_{44}^D value and that determined using the UPE method

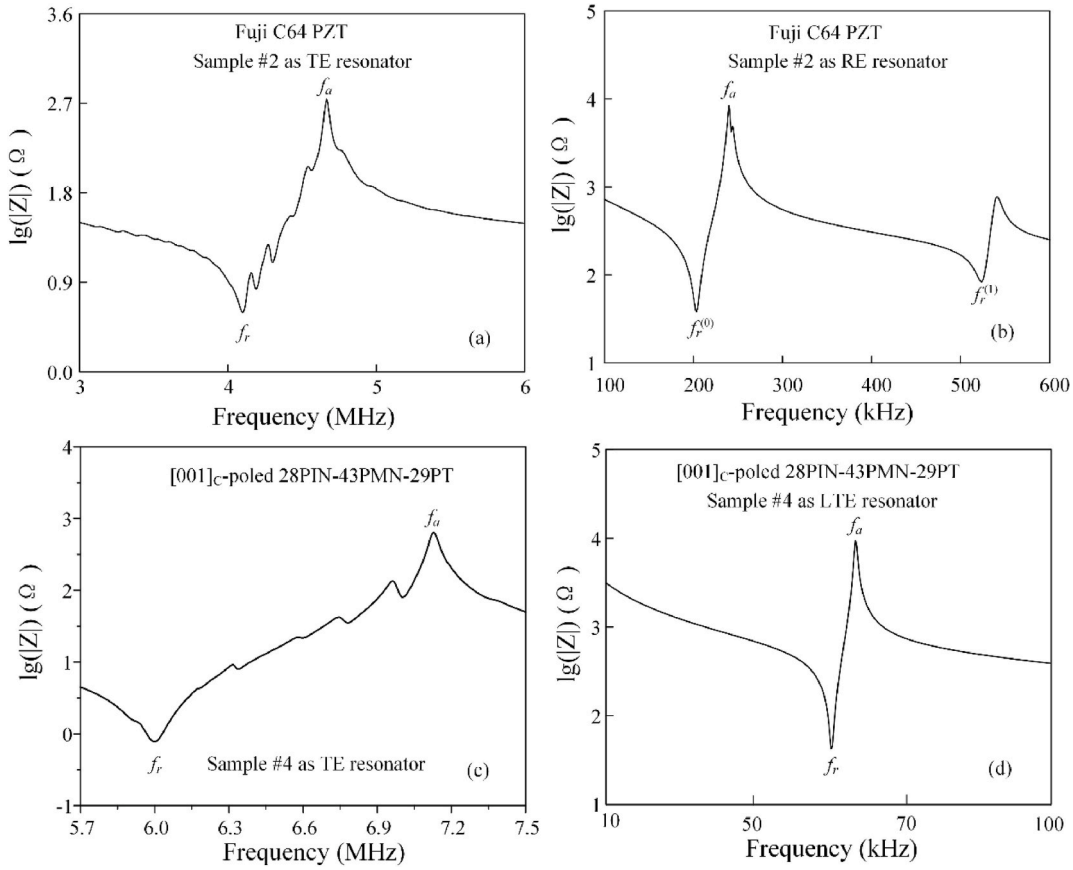

Fig. 5. Electric impedance spectra of Fuji C64 PZT disk sample (#2) and $[001]_C$-poled 28PIN-43PMN-29PT single crystal long thin slice sample (#4). (a) Sample #2 as TE resonator; (b) Sample #2 as RE resonator; (c) Sample #4 as TE resonator; (d) Sample #4 as LTE resonator.

Table 3
Full matrix material constants of the Fuji C64 PZT sample.

c_{ij}^E (10^{10} N/m^2)					c_{ij}^D (10^{10} N/m^2)				
c_{11}^E	c_{12}^E	c_{13}^E	c_{33}^E	c_{44}^E	c_{11}^D	c_{12}^D	c_{13}^D	c_{33}^D	c_{44}^D
12.78	8.220	8.320	11.92	1.982	13.16	8.599	7.043	15.54	3.959
s_{ij}^E (10^{-12} m^2/N)					s_{ij}^D (10^{-12} m^2/N)				
s_{11}^E	s_{12}^E	s_{13}^E	s_{33}^E	s_{44}^E	s_{11}^D	s_{12}^D	s_{13}^D	s_{33}^D	s_{44}^D
16.83	−5.897	−7.437	18.77	50.45	14.16	−7.769	−2.773	8.568	26.00
e_{ij} (C/m^2)					d_{ij} (10^{-12} C/N)				
e_{15}	e_{31}		e_{33}		d_{15}	d_{31}		d_{33}	d_h
12.58	−5.51		18.50		635	−197		431	37
g_{ij} (10^{-3} Vm/N)					h_{ij} (10^8 V/m)				
g_{15}	g_{31}		g_{33}		h_{15}	h_{31}		h_{33}	
39.7	−10.8		23.7		14.81	−6.87		23.18	
ϵ_{ij}^T (ϵ_0)		ϵ_{ij}^S (ϵ_0)			β_{ij}^T ($10^{-4}/\epsilon_0$)			β_{ij}^S ($10^{-4}/\epsilon_0$)	
ϵ_{11}^T	ϵ_{33}^T	ϵ_{11}^S	ϵ_{33}^S		β_{11}^T	β_{33}^T		β_{11}^S	β_{33}^S
1802	1880	960	906		5.537	4.864		10.42	11.04
k_{ij}									
k_{15}	k_{31}	k_{33}	k_t	k_p		σ^E			
0.70	0.36	0.74	0.51	0.65		0.35			

(Table 3) was approximately 2.9 %.

The calculated c_{33}^D and c_{44}^D values of the $[001]_C$-poled 28PIN-43PMN-29PT single crystals were 16.778 × 10^{10} and 7.656 × 10^{10} N/m^2, respectively. The relative errors between the calculated c_{33}^D values and those obtained using the UPE method (Table 4) and the ER method (16.775 × 10^{10} N/m^2) were approximately 1.2 % and 0.02 %, respectively. Moreover, the relative error between the calculated c_{44}^D value and that determined using the UPE method (Table 4) was approximately 3.3 %.

The results were further evaluated by comparing the measured

Table 4
Full matrix material constants of the $[001]_C$-poled 28PIN-43PMN-29PT sample.

c_{ij}^E (10^{10} N/m^2)						c_{ij}^D (10^{10} N/m^2)					
c_{11}^E	c_{12}^E	c_{13}^E	c_{33}^E	c_{44}^E	c_{66}^E	c_{11}^D	c_{12}^D	c_{13}^D	c_{33}^D	c_{44}^D	c_{66}^D
11.43	9.988	9.782	11.14	6.492	6.049	11.82	10.37	8.298	16.58	7.411	6.049
s_{ij}^E (10^{-12} m^2/N)						s_{ij}^D (10^{-12} m^2/N)					
s_{11}^E	s_{12}^E	s_{13}^E	s_{33}^E	s_{44}^E	s_{66}^E	s_{11}^D	s_{12}^D	s_{13}^D	s_{33}^D	s_{44}^D	s_{66}^D
46.28	−22.69	−20.71	45.35	15.404	16.53	38.06	−30.90	−3.538	9.460	13.06	16.53
e_{ij} (C/m^2)						d_{ij} (10^{-12} C/N)					
e_{15}		e_{31}		e_{33}		d_{15}		d_{31}	d_{33}	d_h	
9.92		−5.10		19.4		161		−568	1178	41	
g_{ij} (10^{-3} Vm/N)						h_{ij} (10^8 V/m)					
g_{15}		g_{31}		g_{33}		h_{15}		h_{31}		h_{33}	
12.54		−15.87		33.15		11.73		−7.639		29.06	
ε_{ij}^T (ε_0)		ε_{ij}^S (ε_0)				β_{ij}^T ($10^{-4}/\varepsilon_0$)			β_{ij}^S ($10^{-4}/\varepsilon_0$)		
ε_{11}^T		ε_{33}^T	ε_{11}^S	ε_{33}^S		β_{11}^T		β_{33}^T	β_{11}^S	β_{33}^S	
1376		3990	955	754		8.879		2.669	10.47	13.26	
k_{ij}											
k_{15}		k_{31}	k_{33}	k_t							
0.39		0.42	0.89	0.58							

electric impedance spectra of samples #1 and #3 with those calculated using the finite-element method and the FMMCs shown in Tables 3 and 4 The measured and calculated electric impedance spectra of the Fuji C64 PZT sample (#1) and the $[001]_C$-poled 28PIN-43PMN-29PT single crystal sample (#3) are shown in Fig. 6. The measured and calculated electric impedance spectra were consistent, demonstrating the reliability of the results and the feasibility of the method presented in this study.

4. Conclusion

The EPCs of PMs with ∞mm and 4mm point group symmetries were characterized using a combination of the ultrasonic pulse-echo method, electric resonance method, and d_h measurement. The characterization procedure consisted of the following steps: i) The dielectric constants $\{\varepsilon_{11}^T, \varepsilon_{33}^T, \varepsilon_{11}^S, \varepsilon_{33}^S\}$ of a rectangular block sample were measured using an impedance analyzer; ii) The elastic constants $\{c_{11}^E, c_{66}^E, c_{33}^D, c_{44}^E, c_{44}^D\}$ of the rectangular block sample were characterized using the UPE method. The c_{12}^E value of the sample with ∞mm point group symmetry was calculated as $c_{12}^E = c_{11}^E - 2c_{66}^E$; iii) The piezoelectric constants d_{15} and e_{15} were calculated using Eqs. (9) and (10), respectively; iv) Disks and long thin slice samples of the PMs with ∞mm and 4mm point group symmetries, respectively, were used as TE resonators, and $\{k_t, c_{33}^D, c_{33}^E, e_{33}\}$ were characterized using the ER method; v) The disk sample of PMs with ∞mm point group symmetry was used as an RE resonator, and $\{\sigma^E, s_{11}^E, s_{12}^E, k_p, k_{31}, d_{31}\}$ were characterized using the ER method. The long thin slice sample of the PMs with 4mm point group symmetry was used as an LTE resonator, and $\{s_{11}^E, k_{31}, d_{31}\}$ were characterized using the ER method; vi) d_h was measured using the block sample, and d_{33} was calculated using $d_{33} = d_h - 2d_{31}$; vii) The elastic constant c_{13}^E of the PMs with ∞mm point group symmetry was characterized by comparing the calculated s_{11}^E and s_{12}^E values with those obtained from the RE resonator using the ER method. e_{31} was then characterized using Eq. (28). The e_{31}, c_{13}^E and c_{12}^E values of the PMs with 4mm point group symmetry were characterized using Eqs. (29)–(31), respectively. The e_{31} and c_{13}^E values of the PMs with 4mm point group symmetry can also be characterized using Eqs. (29) and (30), respectively; ix) Other material constants were calculated using equations that express the relationship between different constants.

By measuring d_h, the LE resonator, which is used for characterizing d_{33} in ER, is no longer needed. The piezoelectric constants d_{15} and e_{15} can be characterized using Eqs. (9) and (10), respectively, and the elastic constants c_{44}^E and c_{44}^D can be characterized using UPE. The thickness

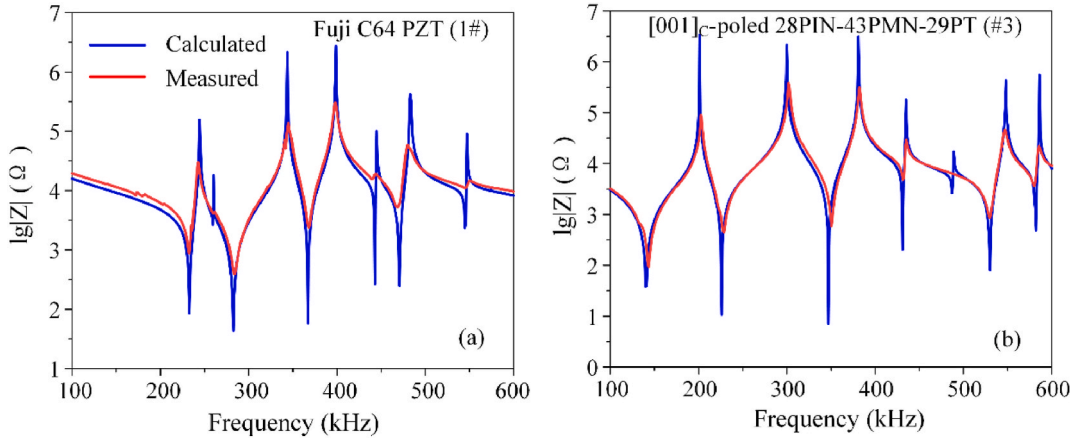

Fig. 6. Measured and calculated electric impedance spectra. (a) Fuji C64 PZT sample (#1); (b) $[001]_C$-poled 28PIN-43PMN-29PT sample (#3).

shear extensional resonator is therefore no longer needed. In addition, the RE and LTE resonators can also be used as TE resonators, further reducing the number of samples required for characterization. The number of samples required to characterize the EPCs of PMs with ∞mm and 4mm point group symmetries were significantly reduced, necessitating the analysis of only two samples rather than the five required by the traditional ER method. The PMs with ∞mm point group symmetry were characterized using only a rectangular block sample and thin-disk sample, while characterization of the PMs with 4mm point group symmetry required only a rectangular block sample and long thin slice sample. Reducing the number of samples used in the characterization of the PMs improves the self-consistency of the results and significantly reduces the sample preparation time. Our findings conclusively demonstrate that the EPCs of PMs with the ∞mm and 4mm symmetries can be accurately determined using the method introduced herein.

CRediT authorship contribution statement

Shanshan Sun: Writing – original draft, Visualization, Investigation, Formal analysis, Data curation. **Youquan Chen:** Writing – original draft, Visualization, Investigation, Formal analysis, Data curation. **Shusheng Li:** Writing – review & editing, Validation, Supervision, Methodology, Investigation, Data curation, Conceptualization. **Ruoyu Jia:** Investigation, Data curation. **Ailing Xiao:** Investigation, Data curation. **Liguo Tang:** Writing – review & editing, Validation, Supervision, Project administration, Methodology, Funding acquisition, Conceptualization. **Wenyu Luo:** Writing – review & editing, Conceptualization.

Declaration of competing interest

The authors declare that they have no known competing financial interests or personal relationships that could have appeared to influence the work reported in this paper.

Acknowledgements

This work was supported by the National Natural Science Foundation of China (Grant No. 12274358); Guangdong Basic and Applied Research Foundation (Grant No. 2024A1515010019); Stable Supporting Fund of Acoustic Science and Technology Laboratory (Grant No. JCKYS2025SSJS011); Open Fund of State Key Laboratory of Acoustics and Marine Information, Chinese Academy of Science (Grant No. SKLA202511); and Open Innovation Fund for undergraduate students of Xiamen University (Grant No. KFJJ-ZD-202403).

References

[1] IEEE Standard on Piezoelectricity, vol. 176, ANSI/IEEE Std, 1987.
[2] R. Benchmann, Elastic, piezoelectric, and dielectric constants of polarized barium titanate ceramics and some applications of the piezoelectric equations, J. Acoust. Soc. Am. 28 (1996) 347–350.
[3] S. Sherrit, H.D. Wiedrick, B.K. Mukherjee, A complete characterization of the piezoelectric, dielectric, and elastic properties of Motorola PZT 3203 HD, including losses and dispersion, Proc. SPIE 3037 (1997) 158–169.
[4] H. Cao, V.H. Schmidt, R. Zhang, W. Cao, H. Luo, Elastic, piezoelectric, and dielectric properties of 0.58Pb($Mg_{1/3}Nb_{2/3}$)O_3-0.42$PbTiO_3$ single crystal, J. Appl. Phys. 96 (2004) 549–554.
[5] L. Qiao, Q. Li, C. Qiu, Y. Liu, J. Liu, Z. Xu, F. Li, Temperature dependence of elastic, piezoelectric, and dielectric matrixes of [001]-Poled rhombohedral PIN-PMN-PT single crystals, IEEE. Trans. Ultrason. Ferroelectr. Freq, Control 66 (2019) 1786–1792.
[6] V.Y. Topolov, Comment on "complete sets of elastic, dielectric, and piezoelectric properties of flux-grown [011]-poled Pb($Mg_{1/3}Nb_{2/3}$)O_3−(28–32)% $PbTiO_3$ single crystals, Appl. Phys. Lett. 92 (2008) 142906. Appl. Phys. Lett. 96 (2010) 196101".
[7] V.Y. Topolov, C.R. Bowen, Inconsistencies of the complete sets of electromechanical constants of relaxor-ferroelectric single crystals, J. Appl. Phys. 109 (2011) 094107.
[8] S. Sheritt, T.J. Masys, H.D. Wiederick, B.K. Mukherjee, Determination of the reduced matrix of the piezoelectric, dielectric, and elastic material constants for a piezoelectric material with C_∞ symmetry, IEEE Trans. Ultrason. Ferroelectrics Freq. Control 58 (2011) 1714–1720.
[9] A. Migliori, J.L. Sarrao, Resonant Ultrasound Spectroscopy, Wiley Press, 1997.
[10] I. Ohno, Rectangular parallellepiped resonance method for piezoelectric crystals and elastic constants of alpha-quartz, Phys. Chem. Miner. 17 (1990) 371–378.
[11] H. Ogi, M. Fukunaga, M. Hirao, H. Ledbetter, Elastic constants, internal friction, and piezoelectric coefficient of α −TeO_2, Phys. Rev. B 69 (2004) 024104.
[12] L.G. Tang, W. Cao, Temperature dependence of self-consistent full matrix material constants of lead zirconate titanate ceramics, Appl. Phys. Lett. 106 (2015) 052902.
[13] C.W. Chen, Y. Xiang, L.G. Tang, X.W. Li, L. Qin, W.W. Cao, Ultrasonic pulse-echo technique for the characterization of elastic constants of single domain Pb($Zn_{1/3}Nb_{2/3}$)O_3–5.5%$PbTiO_3$ single crystals with 3m symmetry, J. Mater. Sci. 55 (2020) 12737–12746.
[14] R. Zhang, B. Jiang, W.W. Cao, Elastic, piezoelectric, and dielectric properties of multidomain 0.67Pb($Mg_{1/3}Nb_{2/3}$)O_3–0.33$PbTiO_3$ single crystals, J. Appl. Phys. 90 (2001) 3471–3475.
[15] G. Liu, W.H. Jiang, J.Q. Zhu, W.W. Cao, Electromechanical properties and anisotropy of single- and multi-domain 0.72Pb($Mg_{1/3}Nb_{2/3}$)O_3-0.28$PbTiO_3$ single crystals, Appl. Phys. Lett. 99 (2011) 162901.
[16] A.L. Xiao, L.G. Tang, S.S. Sun, S.J. Wu, X.Y. Wu, W.Y. Luo, Comparison of characterization methods for assessing the temperature dependencies of elastic and piezoelectric constants of piezoelectric materials, IEEE Trans. Instrum. Meas. 72 (2023) 1–15.
[17] https://www.fujicera.co.jp/wpkanri/wp-content/uploads/2024/09/The-material-characteristics-of-piezoceramics_2024.09E.pdf.
[18] E.W. Sun, R. Zhang, F.M. Wu, W.W. Cao, Complete matrix properties of [001]c and [011]c poled 0.33Pb(In1/2Nb1/2)O3-0.38Pb(Mg1/3Nb2/3)O3-0.29PbTiO3 single crystals, J. Alloys Compd. 553 (2013) 267–269.